Available online at www.sciencedirect.com
ScienceDirect
Journal of Power Sources 158 (2006) 1306–1312
JOURNAL OF POWER SOURCES
www.elsevier.com/locate/jpowsour

PEM fuel cell cathode carbon corrosion due to the formation of air/fuel boundary at the anode

Hao Tang, Zhigang Qi *, Manikandan Ramani, John F. Elter

Plug Power Inc., 968 Albany Shaker Road, Latham, NY 12110, USA

Received 29 September 2005; accepted 18 October 2005
Available online 28 November 2005

Abstract

The impacts of unprotected start up and shut down on fuel cell performance degradation was investigated using both single cell and dual cell configurations. It was found that the air/fuel boundary developed at the anode side after a fuel cell shut down or during its restart caused extremely quick degradation of the cathode. The thickness, the electrochemical active surface area, and the performance of the cathode catalyst layer were significantly reduced. By using a dual cell configuration, cathode potential as high as two times of open circuit voltage was measured, and the corrosion current flowing externally between the two cells was detected and quantified. Carbon catalyst-support corrosion/oxidation at such a high potential was largely responsible for the accelerated fuel cell performance degradation.

Keywords: Fuel cell; Fuel cell start up; Fuel cell shut down; Carbon corrosion; Carbon oxidation; Air/fuel boundary; Fuel cell degradation

1. Introduction

Inadequate reliability is one of the primary factors that impede the large-scale commercialization of proton exchange membrane fuel cells [1,2]. Understanding the root causes for various failure modes is crucial to improving the reliability. Electrochemical reactions occur within the membrane–electrode assembly, and thus, the latter is a key component of a fuel cell. Its durability is affected by both its physical properties and the fuel cell operating conditions.

The state of the art fuel cell electrode is normally composed of carbon-supported noble metal catalyst such as Pt, an ionic conductor such as Nafion, and a water-repelling agent such as PTFE [3,4]. The carbon support provides several desired functions. First, it enables the uniform dispersion of Pt nanoparticles. Second, it retards the sintering or agglomeration of Pt nanoparticles. Third, it provides electronic continuity.

Carbon as a support has good chemical and electrochemical stabilities, and these properties make it popular fuel cell catalyst-support. However, carbon will be oxidized/corroded at potentials near the open circuit voltage (OCV) of a fuel cell (about 1.0 V), and the oxidation rate increases with the potential. The presence of Pt could accelerate the carbon corrosion rate [5], and the corrosion may be more severe at places where Pt particles reside. This would weaken the attachment of Pt particles to the carbon support, and even eventually lead to the detachment of Pt particles from the carbon support, resulting in quicker Pt particle agglomeration. In addition, the loss of carbon due to its corrosion could decrease the electronic continuity of the catalyst layer, and isolated Pt particles would not be able to participate in the electrochemical reactions.

Under normal fuel cell operations, the highest potential that the cathode encounters will be the OCV, which is 1.0 V or slightly lower. For most of the time, the fuel cell will have a load, and the cathode voltage is likely to be between 0.4 and 0.7 V. At such potentials, the carbon corrosion will not be severe, and it should have limited impact on the durability. However, after the fuel cell shut down or during its restart, some portions of the cathode could experience a potential as high as twice of the OCV. Such a high potential would quickly corrode the carbon catalyst-support [6–9].

Fig. 1 shows what could happen after an unprotected fuel cell shut down. After the shut down, there will be unreacted air and hydrogen at the cathode and anode, respectively, resulting in an OCV of about 1.0 V. If the anode exhaust port is not closed after shut down, air will gradually diffuse into the anode side,

* Corresponding author. Tel.: +1 518 738 0229; fax: +1 518 782 7914.
E-mail address: zhigang_qi@plugpower.com (Z. Qi).

0378-7753/$ – see front matter © 2005 Elsevier B.V. All rights reserved.
doi:10.1016/j.jpowsour.2005.10.059

creating an air/hydrogen boundary, represented by the dotted line, and the boundary moves to the other end of the flow channel. The boundary line creates four distinct regions marked A–D. Both regions B and C are connected with region A through the membrane, and thus they will bear a potential of OCV. At the same time, since the entire cathode is about 1.0 V higher than the entire anode, the potential of region D will be close to the sum of the potentials at regions B and C, which is about two times of OCV. Please note that all the potentials mentioned here refer to the potential difference between the electrode and the membrane electrolyte; and the potential of the membrane electrolyte section shared by regions A and B could be largely different from that shared by regions C and D. At such a high potential, both water electrolysis and carbon oxidation could happen in region D at significant rates according to Eqs. (1)–(3):

$$2H_2O \rightarrow O_2 + 4H^+ + 4e^- \quad (1)$$

$$C + 2H_2O \rightarrow CO_2 + 4H^+ + 4e^- \quad (2)$$

$$C + O_2 \rightarrow CO_2 \quad (3)$$

The surface of Pt particles could also be oxidized according to Eqs. (4) and (5):

$$Pt + xH_2O \rightarrow PtO_x + 2xH^+ + 2xe^- \quad (4)$$

$$Pt + xO_2 \rightarrow PtO_{2x} \quad (5)$$

Resulting from the reactions occurring in regions A–D, there will be electron flows between regions A and C, and between regions B and D, as well as proton flows between regions A and B, across the dotted line, and between regions C and D, as shown in Fig. 1 (reactions (3)–(5) and proton movement across the dotted line are not shown in Fig. 1 for simplicity).

The boundary will disappear after all the hydrogen is consumed or displaced, and the anode will be filled with air eventually. The high potential region D will then disappear, and reactions (1)–(5) will stop or proceed with much less severity. However, when hydrogen is fed to the anode during the restart of the fuel cell, a new air/fuel boundary forms, causing cathode in the region that faces the anode air section to corrode according to reactions (1)–(5).

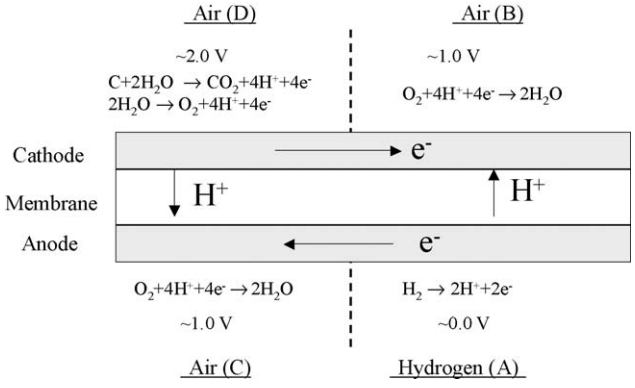

Fig. 1. A schematic illustration of reactions in four distinct regions when an air/fuel boundary is formed at the anode. Region D experiences a potential of about twice of the OCV, and thus carbon in that region would be corroded quickly.

Colleagues at UTC Fuel Cells have done some excellent work in this area for the past several years [6–9]. A recent publication by Reiser et al. modeled this phenomenon using a simplified mathematical approach and obtained the electrolyte potential profile. Fuel cell performance degradation and cathode catalyst layer thinning were also investigated [9].

This phenomenon was also observed and studied at Plug Power in the past several years. By using a dual cell configuration, we were able to detect and quantify the external corrosion current between the two cells caused by the formation of air/hydrogen boundary, and thus it directly validated the corrosion process.

2. Experimental

2.1. Fuel cell performance

Single fuel cell tests were performed using a homemade 50 cm^2 active area test fixture. The test fixture was composed of a pair of graphite plates with serpentine flow-fields for the reactants to flow. There are cooling channels on the back of the plates for liquid water to flow. Rod-like heaters were inserted into the plates to help control the cell temperature.

Reformate and air were used as the reactants at the anode and cathode, respectively. A 2% air bleed was used at the anode side to enhance the CO tolerance [10]. The reformate was composed of 10 ppm CO, 49% H_2, 17% CO_2, and balanced by N_2. The cell temperature was controlled at 65 °C, and both reactants were 100% humidified by passing them through humidifiers prior to allowing them to enter the cell.

2.2. Cyclic voltammetry (CV)

An EG&G Potentiostat (Model 263 A) was used to perform the cyclic voltammetry. When the CV of the cathode (or anode) was measured, it was taken as a working electrode, and was fed with an inert gas such as nitrogen; while the anode (or cathode) was fed with pure hydrogen and it functioned as the counter and reference electrode. Both gases were 100% humidified at the cell temperature. The potential was scanned at 20 mV s^{-1} between 0.05 and 0.50 V.

2.3. Scanning electron microscopy (SEM)

A JEOL 6400 instrument was used for SEM analysis in order to evaluate the cross section thickness of an MEA. The SEM sample was prepared by first freezing it using liquid nitrogen before breaking it at the desired locations.

3. Results and discussion

3.1. Single cell configuration

Fig. 2 schematically shows the setup of a single cell configuration for the investigation of cathode corrosion. Air was continuously fed to the cathode, while reformate and air were fed to the anode alternatively and repeatedly. When reformate

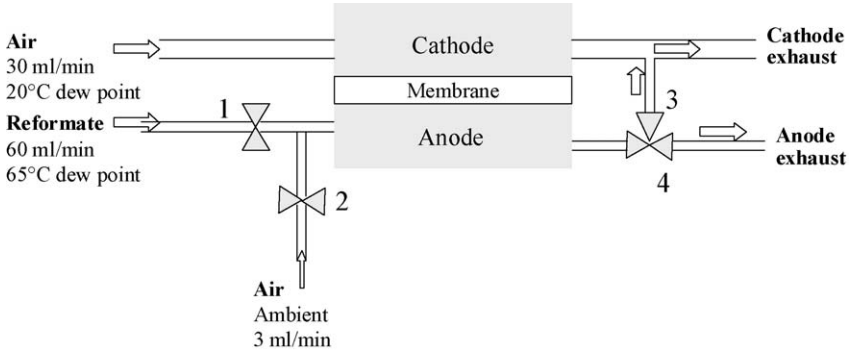

Fig. 2. Single cell configuration.

was fed to the anode, valves 1 and 4 were opened, and valves 2 and 3 were closed. When air was fed to the anode, valves 1 and 4 were closed, and valves 2 and 3 were opened. The flow rates of both the reformate and air to the anode were carefully controlled in this process. Please note that the air was kept at ambient condition (i.e. ambient temperature and humidity) and the reformate was fully humidified during this corrosion process. The fuel cell performance and the physical properties of the cathode were evaluated periodically after different number of corrosion cycles, and fully humidified gases were used.

The cell open circuit voltage change during eight cycles of corrosion process is illustrated in Fig. 3. When the reformate was switched off and air was fed to the anode side, it triggered a steep decline in OCV and it reached to ca. 0.1 V in several minutes. When air was switched off and reformate switched on, the OCV jumped to ca. 1.1 V initially, and it then declined gradually. When OCV declined to about 0.90 V, air was fed to the anode again. Feeding reformate and air to the anode was alternated and repeated.

Fig. 4 shows the fuel cell performance at the beginning-of-life, and after 20, 40, and 80 cycles of corrosion processes. The flow rates of the reformate and air were controlled constant at 1.2 and 2.0 times stoichiometric for a current density of 0.60 A cm^{-2}, respectively, and 2% air bleed was used at the anode. A large performance drop was observed after 20 cycles, and the performance drop continued as the number of cycles increased, but the decline rate became slower.

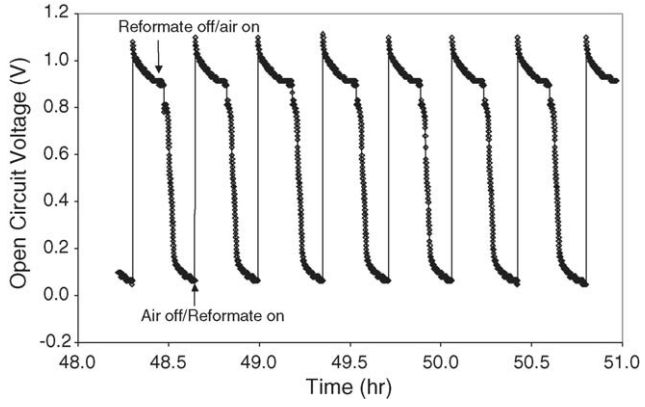

Fig. 3. Cell OCV change when air and reformate are alternatively fed to the anode.

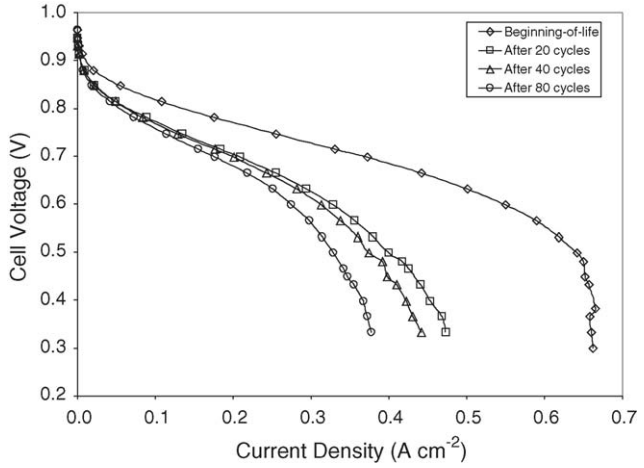

Fig. 4. Effect of corrosion cycles on fuel cell performance; 65 °C cell temperature; cathode: air, 100% RH; anode: reformate with 2% air bleed, 100% RH.

Obviously, the corrosion process severely reduced the fuel cell performance.

Hydrogen adsorption and desorption peak areas were used to estimate the electrochemical active surface area of the cathode, and the result is plotted in Fig. 5. Clearly, the cathode lost tremendous amount of active surface area in 80 cycles. The quickest decline occurred within about the first 30 cycles, and it approached a stabilization level after about 80 cycles.

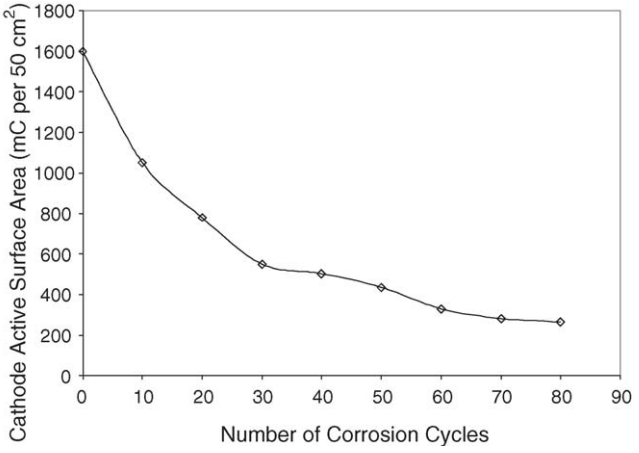

Fig. 5. Effect of corrosion cycles on cathode electrochemical active surface area.

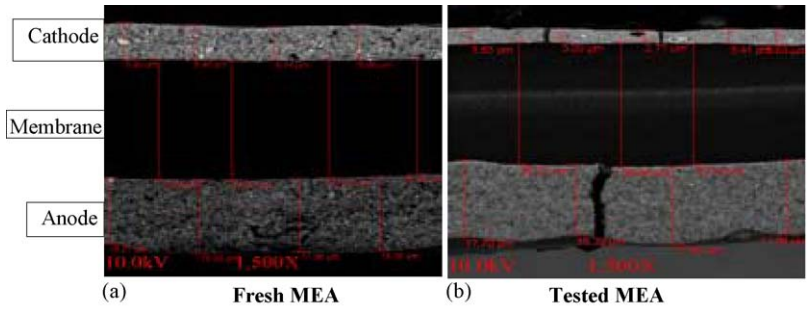

Fig. 6. SEM of fresh (a) and tested MEAs after 80 cycles (b); magnification 1500×.

This decline trend agreed well with the performance degradation trend shown in Fig. 4.

Scanning electron spectroscopy was used to measure the thickness of the catalyst layers, and the results are shown in Fig. 6. Compared to the fresh MEA shown in Fig. 6a, the cathode catalyst layer thickness was reduced to about 1/3 of its original value after 80 cycles, while the anode thickness did not show much change (Fig. 6b). So, the carbon catalyst-support in the cathode was severely corroded away.

3.2. Dual cell configuration

As shown in Fig. 1, there should be electron flows between regions A and C, and between regions B and D during the corrosion process due to the formation of air/fuel boundary at the anode. However, it is not possible to detect the electron flows by using the single cell configuration shown in Fig. 2. A configuration that can spatially separate region A from C, and B from D will be needed in order to detect and measure some of the corrosion current.

Fig. 7 shows a dual cell configuration that meets such a requirement to some degree. It consists of two single cells that are connected both physically and electrically. Cells 1 and 2 were physically connected by conducting cell 1's anode and cathode exhausts to cell 2's anode and cathode inlets, respectively. Cells 1 and 2 were electrically connected by linking the two cathode current collectors together using a metal wire and the two anode current collectors together using an multi-channel HP Agilent 34401A digital multimeter, respectively. The digital multimeter was connected to a real time data acquisition system programmed by Lab-View, and it allowed continuous measurement of the current between anodes 1 and 2. When air flowed through these compartments that was initially filled with reformate, we refer it as Case 1. When reformate flowed through the anode compartments that was initially filled with air, we refer it as Case 2. The cell 1 voltage was measured through a data acquisition system and hence continuous data were available; while cell 2 voltage was measured at discrete times using a voltmeter. The flow rates and the relative humidity levels of the gases are detailed in the figure.

In order to estimate the potential of cell 2 cathode, cells 1 and 2 were initially not connected either physically or electrically. Air and reformate were fed through cell 1 cathode and anode, respectively, and were vent out to exhaust lines directly. This cell showed a voltage of 0.93 V (cathode 1 versus anode 1). At the same time, both the anode and cathode of cell 2 were filled with air, and this cell showed a voltage of 0 V (cathode 2 versus anode 2). Since cell 2 anode was filled with air, its potential versus cell 1 anode potential should be around 0.93 V. Once electrical connections were made between cells 1 and 2, cell 2 voltage rose to 0.82 V immediately. This essentially meant to us that cell 2 cathode potential increased to about 1.75 V versus cell 1 anode. These measured values are shown in Fig. 7.

Fig. 8 shows the cell 1 voltage change and the current flow between anodes 1 and 2 in one cycle. When air entered cell 1 anode that was initially filled with reformate, cell 1 voltage started to go down towards 0.1 V (Case 1 region). A current flow from cell 1 anode to cell 2 anode was detected (note that

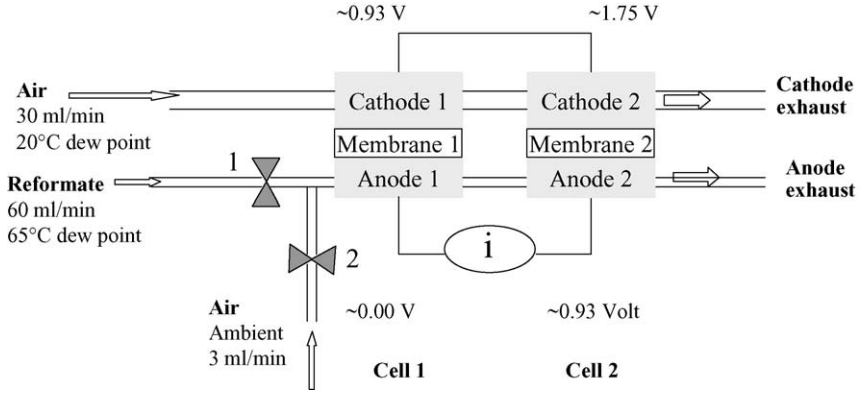

Fig. 7. Dual cell configuration.

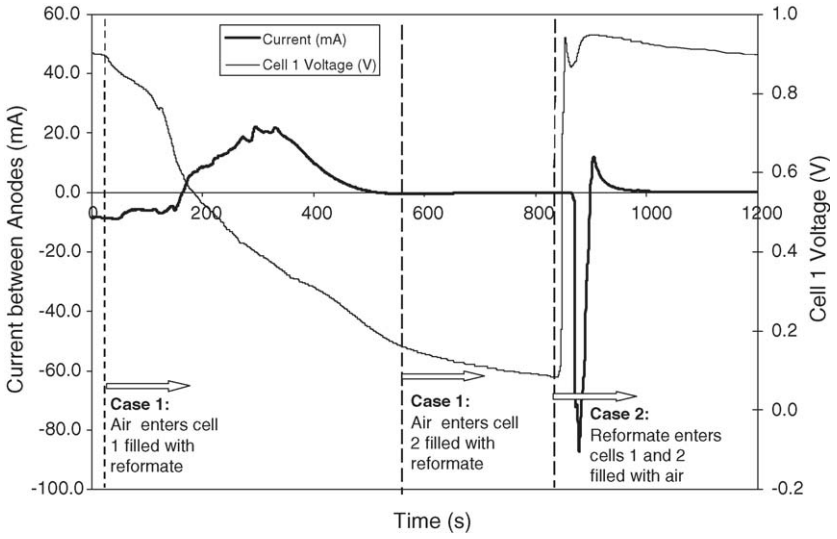

Fig. 8. Profiles of cell 1 voltage and the current between the anodes of cells 1 and 2 when air and reformate are fed to the anodes alternatively.

the electrons flowed from cell 2 anode to cell 1 anode), and a current peak of around 20 mA was observed. Once cell 1 anode was completely filled with air, the current flow between anodes 1 and 2 disappeared completely. Air then entered cell 2 anode, and no current flow between the two anodes was generated.

Without waiting for air to flow through cell 2 anode completely, Case 2 was started by flowing the reformate to cell 1 anode and then cell 2 anode. Cell 1 voltage jumped up beyond 0.9 V immediately after the reformate entered cell 1 anode. Since the reformate flow rate was much higher than the air flow rate (60 ml min^{-1} versus 3 ml min^{-1}), a very sharp current peak of about 88 mA was observed, and the current flow direction was from cell 2 anode to cell 1 anode. This current died down quickly once cell 1 anode was completely filled with the reformate. Surprisingly, when the reformate entered cell 2, a smaller and reversed transient current flow from cell 1 anode to cell 2 anode was observed. We have no good explanation to this reversal current yet. Once the reformate filled cell 2 anode, the current between cells 1 and 2 anodes completely disappeared.

The electrochemical active surface area of cell 2 cathode was measured to be about 35% of the initial value after 50 such cycles (Fig. 9, filled square). Fig. 9 also shows the correlation between electrochemical active surface area and cell voltage at a current density of 0.1 A cm^{-2} of another identical MEA. This MEA was galvanically corroded using an external power sources at a galvanic current density of 2 mA cm^{-2}, and its performance and the cathode electrochemical active area were measured periodically. The performance and the cathode electrochemical active surface area of cell 2 agreed well with this galvanically corroded cell.

Integrating the currents with time observed in the dual cell configuration yielded a total charge of about 8.0 C per cycle (switching between reformate and air). Out of this total charge, approximately 6.0 C (75%) came from Case 1 where air entered the anodes that were filled with reformate, and 2.0 C (25%) came from Case 2 where reformate entered the anodes that were filled with air. This amount of charge could corrode 0.25 mg of carbon when C is oxidized to CO_2 according to Eq. (2) (8.0×12–$96{,}500$–4×1000 mg). If we assume that the cathode catalyst layer contained about 0.6 mg cm^{-2} carbon as the catalyst-support, two 50 cm^{-2} cells will have a total carbon loading of 60 mg. Thus, the carbon corroded per cycle by this amount of charge was about 0.4% of the total carbon in the catalyst layer (=0.25 mg/60 mg).

It is interesting to notice that Case 1 caused more corrosion to the cathode than Case 2 (6 C versus 2 C corrosion charge). This was probably because air was fed to the anodes (Case 1) at a much slower rate than reformate (Case 2), so that the air/fuel boundary lasted much longer in Case 1 than in Case 2. This may imply that by quickly purging the anode after fuel cell shut down or during its restart, the cathode would be corroded less—even an air/fuel boundary forms in these fast purging processes.

The measured current between cells 1 and 2 might account only a portion of the total corrosion current occurring at cathodes 1 and 2. As shown in Fig. 10, the total corrosion current is the sum of the internal current I_1 and the external current I_2. What we

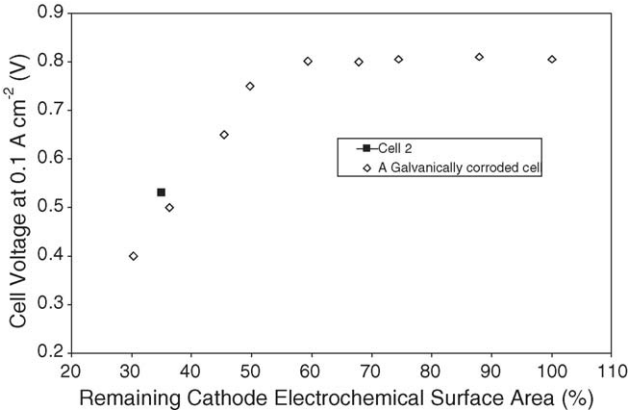

Fig. 9. Cathode electrochemical active surface area vs. fuel cell voltage at 0.1 A cm^{-2} for a galvanically corroded cell (open diamond). The filled square represents cell 2 cathode after 50 corrosion cycles in the dual cell configuration.

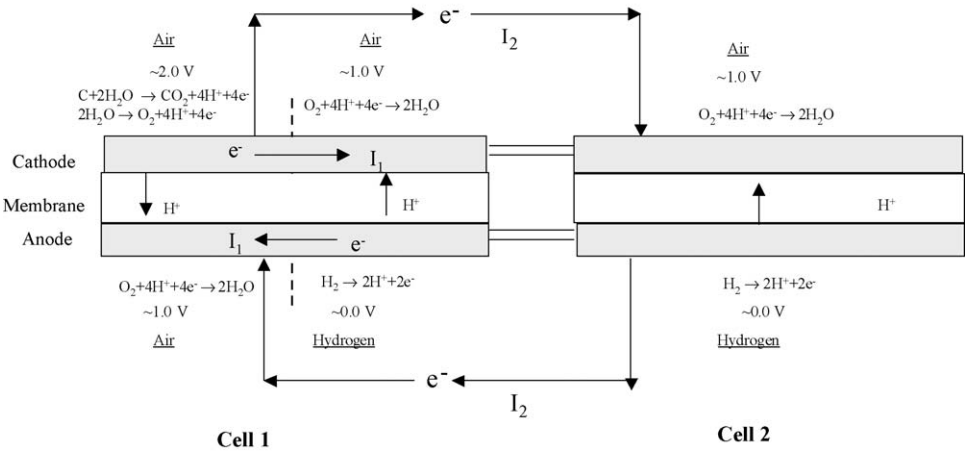

Fig. 10. A schematic illustration of internal and external corrosion currents in the dual cell configuration.

were able to measure was only I_2. Since the electrode materials are very good electron conductors, I_1 should not encounter much resistance to against the flow of electrons; and thus, it could be significant too. By comparing the results from the single cell and dual cell experiments, we could make an estimate about their relative contributions to the cathode corrosion in the dual cell configuration.

In the single cell experiments, the cathode catalyst layer thickness was reduced to about 1/3 of its virgin thickness after 80 cycles (Fig. 6). Although we were not sure exactly how much carbon was corroded away, it would be certain that at least 2/3 of the carbon was corroded away based on the thickness reduction and the following reasoning. One other component within the catalyst layer is Nafion, and its content normally ranges from 20 to 30% by weight, translating to a volume fraction of approximately 20–30%. The high voltage might also cause some damage to Nafion, but its loss from the catalyst layer should be minimal. Some Pt might be dissolved due to the high voltage, but the volume taken by Pt is much less than either carbon or Nafion. So, if carbon takes 70–80% volume fraction within the catalyst layer, and its corrosion is the primary reason to cause the catalyst layer thickness to reduce for 2/3, the loss of carbon must be least 2/3 of its initial amount. This amount of loss would correspond to about 0.9% of carbon corroded per cycle ((2/3)–80). Therefore, the internal current I_1 was estimated to be about twice of the external current I_2 in the dual cell configuration (0.9%–0.4%).

The total corrosion current $I_1 + I_2$ should also include the contribution from water electrolysis according to Eq. (1). We used very low cathode dew point (20 °C) in the experiments in order to minimize reaction (1) and to maximize reaction (2). The current $I_1 + I_2$ could also cause Pt oxidation and even dissolution. However, water electrolysis and Pt oxidation were not included in the above analysis because their contributions were difficult to quantify.

The above experiments have clearly demonstrated the severity of cathode catalyst layer corrosion when an air/fuel boundary is formed at the anode during unprotected fuel cell shut down and restart. Actions must be taken to prevent such a boundary from formation in order to achieve a long fuel cell life. One approach could be purging both the anode and cathode using an inert gas after the fuel cell is shut down or before the fuel cell is restarted. Another approach could be connecting a suitable resistor to the fuel cell so that the cathode potential would be never higher than OCV during the start up or shut down. A third approach could be using high corrosive resistant materials as the catalyst-supports or completely eliminating the support. However, the high potential could still severely oxidize Pt or other catalysts, leading to either oxide formation or catalyst dissolution.

4. Conclusions

It has been demonstrated that the formation of air/hydrogen boundary at the anode could seriously and quickly corrode the carbon catalyst-support in the cathode, resulting in dramatic catalyst active surface area loss and the fuel cell performance loss. The most sever damage was done within the first 30 cycles when air and fuel were fed to the anode alternatively. After about 50 such cycles, the cathode remained about 30% of its initial electrochemical active surface area; and after 80 such cycles, the cathode catalyst layer thickness was reduced to about 1/3 of its initial value. By using a dual cell configuration, a portion of the corrosion current was able to be detected and quantified. This measured external corrosion current was slightly less than 1/2 of the total corrosion current. Prevention of such an air/fuel boundary from formation during the shut down and restart of a fuel cell is crucial in order to achieve long MEA life.

Acknowledgments

Many thanks to Mr. Mike Knussman for performing the SEM analysis and to Mr. Lam Wong for suggesting the dual cell setup. The authors are grateful to Ms. Cynthia Mahoney White and Mr. Daniel Beaty for their critical review.

References

[1] A.S. Feitelberg, J. Stathopoulos, Z. Qi, C. Smith, J.F. Elter, J. Power Sources 147 (2005) 203–207.

[2] D.P. Wilkinson, J. St-Pierre, Durability, in: W. Vielstich, A. Lamm, H.A. Gasteiger (Eds.), Handbook of Fuel Cells—Fundamentals Technology and Applications, vol. 3, John Wiley & Sons, 2003, pp. 611–626.
[3] E.A. Ticianelli, C.R. Derouin, A. Redondo, S. Srinivasan, J. Electrochem. Soc. 135 (1988) 2209–2214.
[4] M.S. Wilson, S. Gottesfeld, J. Electrochem. Soc. 139 (1992) L28–L30.
[5] D.A. Stevens, J.R. Dahn, Carbon 43 (2005) 179–188.
[6] L.L. Van Dine, M.M. Steinbugler, C.A. Reiser, G.W. Scheffler, U.S. Patent 6,514,635 (2003).
[7] D.A. Condit, R.D. Breault, U.S. Patent 6,635,370 (2003).
[8] T.A. Bekkedahl, L.J. Bregoli, R.D. Breault, E.A. Dykeman, J.P. Meyers, T.W. Patterson, T. Skiba, C. Vargas, D. Yang, J.S. Yi, U.S. Patent 6,913,845 (2005).
[9] C.R. Reiser, L. Bregoli, T.W. Patterson, J.S. Yi, J.D. Yang, M.L. Perry, T.D. Jarvi, Electrochem. Solid-State Lett. 8 (2005) A273–A276.
[10] S.D. Gottesfeld, U.S. Patent 4,910,099 (1990).